TOWARDS UNCERTAINTY QUANTIFICATION OF THE ONERA 7A ROTOR USING COMPREHENSIVE ANALYSIS

Itham Salah El Din , itham.salah_el_din@onera.fr, ONERA The French Aerospace Lab, FRANCE
Manas Khurana, Science and Technology Corporation, Moffett Field, CA, USA
Hyeonsoo Yeo, U.S. Army CCDC-AvMC, Moffett Field, CA, USA

Abstract
The uncertainty and sensitivity of rotor blade torsion stiffness on rotor power and maximum torsion moment is studied. Comprehensive analysis tools are used to establish rotor performance and structural loads. A global-based uncertainty propagation scheme was applied using a scaling factor to uniformly induce spanwise variability in blade torsion stiffness using Monte Carlo simulations. A local-based uncertainty propagation scheme was also applied with a third-order polynomial function to induce a non-uniform distribution of material stiffness. The analysis confirmed that uncertainty in torsion stiffness has negligible impact on rotor power and maximum amplitude torsion moment along the blade span for the considered high-speed case. The analysis does confirm a pronounced effect on half peak-to-peak torsion moment at specific blade span stations where experimental measurements are available. Additionally, a sensitivity analysis using a non-uniform distribution approach with a scaling factor facilitated a comprehensive quantification of the direct and interaction effects between the uncertain parameters on the response outputs.

1. SYMBOLS AND ABBREVIATIONS

CA	Comprehensive Analysis
CDF	Cumulative Distribution Function
CFD	Computational Fluid Dynamics
CI	Confidence Interval
CP	Control Point
GSA	Global Sensitivity Analysis
HOST	Helicopter Overall Simulation Tool
HPP	Half Peak-to-Peak
LHS	Latin Hypercube Sampling
MC	Monte Carlo
MoE	Margin-of-error
PDF	Probability Density Function
Pr.	Probability
RCAS	Rotorcraft Comprehensive Analysis System
RSM	Response Surface Model
SA	Sensitivity Analysis
SF	Scaling Factor
stdev	Standard deviation
TM	Torsion Moment
UQ	Uncertainty Quantification
μ	Advance ratio
σ	Solidity
C_L/σ	Rotor lift coefficient over solidity
Ɲ	Normal distribution

2. INTRODUCTION

The work outlines the role of uncertainty quantification (UQ) for rotorcraft aeromechanics using comprehensive analysis (CA) codes, HOST [1] and RCAS [2]. Respectively ONERA and the U.S. Army have formed and executed a collaborative program to address the research goals on this subject. To support this effort, a computational framework is developed for large-scale analysis using automated processes and methods in a high performance computing environment. The architecture facilitates parametric analysis of complex rotorcraft configurations including the quantification of system uncertainties and sensitivities. The workings of the proposed method and principles are demonstrated on the ONERA 7A rotor as acceptable body-of-knowledge exists with these geometries, and due to the availability of existing databases which have been formed and shared between ONERA and U.S. Army through ongoing research ventures.

In this process, the uncertainties in blade material properties on rotor performance and blade structural loads is established using Monte Carlo (MC) simulations with RCAS and HOST. It is shown that uncertainties in blade torsional stiffness result in variability in total rotor power and maximum half peak-to-peak structural loads. The demonstrated case study further validates that the developed framework is capable of evaluating complex relationships for uncertainty and sensitivity analysis between structural inputs and performance and loads outputs. The knowledge gained from a UQ process is critical to support program decision

Presented at 47th European Rotorcraft Forum, United Kingdom, 7-9th September, 2021
This work is licensed under the Creative Commons Attribution International License (CC BY). Copyright © 2021 by author(s).
DISTRIBUTION STATEMENT A. Approved for public release; distribution is unlimited.

making in planned rotorcraft acquisition programs.

3. BACKGROUND

The CA tool chains are widely used for rotorcraft performance and loads assessment. In this domain, consideration of system uncertainties and sensitivities on established output using deterministic methods needs to be established. Access to this critical information will facilitate capabilities in both model knowledge including risk management and mitigation. The UQ and propagation process through a CA tool chain will provide reliable data for comparison with experimental and/or flight data and will also give access to robust design capabilities.

The Rotorcraft Comprehensive Analysis System (RCAS) [2] and HOST [1] solver codes are used in the calculation of rotor power and blade structural loads. RCAS, developed by the U.S. Army, is a comprehensive multidisciplinary, computer software system that is used for predicting rotorcraft aerodynamics, performance, stability and control, aeroelastic stability, loads, and vibration. Alternately, the Helicopter Overall Simulation Tool (HOST) by Airbus Helicopters is also a rotorcraft comprehensive analysis tool that models blade dynamics using a multibody scheme [3]. The aerodynamics is based on the lifting-line approach that uses airfoil lookup tables combined with an inflow model. In this setup, finite state dynamic inflow model was used for both HOST and RCAS.

In both RCAS and HOST, the structural parameters and corresponding loads are specified and calculated respectively at discrete points along the span. A piecewise linear interpolation scheme is used in RCAS to calculate the values at the intermediate points. The two comprehensive codes are used in this study for the purposes of establishing code-to-code dependencies and to establish the relative influence of the dependencies in uncertainty propagation on a common problem-of-interest. This comparison will further assist ongoing solver development and capability improvement efforts. The study will ultimately define the role of UQ in computational aeromechanics so that methodology benefits when integrated into the available CA tool chains are identifiable. The results will permit the definition of flight performance and load variance envelopes with uncertainties, and this knowledge will facilitate informed decision making through the aircraft design life cycle program.

4. MODEL

The present study focuses on the high-speed condition ($\mu = 0.40$, $C_L/\sigma = 0.063$), which has been investigated by many researchers using various analysis tools and methods [3, 4, 5, 6]. The rotor was trimmed to satisfy the Modane flapping law ($\beta_{1s} = 0$, $\beta_{1c} = -\theta_{1s}$) in addition to the specified rotor lift and propulsive force using rotor collective and cyclic controls and shaft angle. As test model, the ONERA 7A rotor is studied which is a four-bladed fully articulated rotor, with a radius of 2.1m and solidity, σ, of 0.084. The blade is of rectangular planform and uses two airfoils, the OA213 and OA209 as shown in Figure 1. The 7A rotor was extensively tested in the ONERA S1MA transonic wind tunnel.

The ONERA 7A rotor was analyzed in RCAS using 16 nonlinear beam elements and 22 aerodynamic segments.

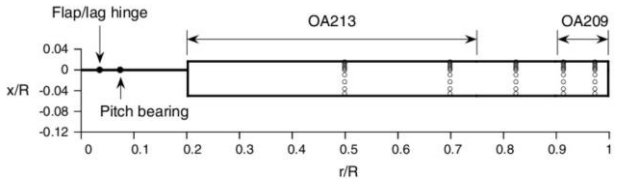

Figure 1: ROTOR 7A blade model definition

The rotor hub was further modeled as fully articulated with pitch bearing and flap and lag hinges. The elastomeric lag damper of the 7A rotor was modeled with equivalent hinge stiffness and damping values at the lag hinge. The lift, drag, and pitching moment on each aerodynamic segments are calculated using airfoil characteristics from C81 lookup tables provided by ONERA. Linear unsteady airloads include classical quasi-steady Theodorsen theory. The finite state dynamic inflow model is used to calculate rotor wake flowfield. A 5.0° (72 steps per rotor revolution) azimuthal step size was used for the trim calculations. In HOST, the 7A rotor blade is modelled using 25 spanwise elements and airfoil lookup tables are used. In this case, the blade is represented as an assembly of rigid segments that are connected by virtual joints. Euler-beam modelling provides three degrees of freedom, namely the chordwise, flapwise, and torsion bending. A 6.0° azimuth step size was imposed for structural dynamic and trim calculations.

A validated inflow model needs to be established as a baseline for the uncertainty analysis to follow. In this setup, the goal was to establish an acceptable balance between computational efficiency and solver accuracy using the proposed CA tools. The present study used the finite-state dynamic inflow model, which was based on the actuator disk solution of the three-dimensional potential flow equations. The induced velocity is expressed in terms of Fourier harmonics (for azimuthal variations) and Legendre functions (for radial variations). In an *m*-by-*n* dynamic inflow model, *m* represents the number of harmonics and *n* represents the highest power in the Legendre

This work is licensed under the Creative Commons Attribution International License (CC BY). Copyright © 2021 by author(s).

polynomials. In the analysis, half peak-to-peak blade structural loads are established as a function of the number of inflow states. Figure 2 compares the RCAS and HOST predictions for torsion moment results with the measured data along the blade span.

Although not shown here, the analysis undertaken confirmed same convergence trends for rotor power. The computational disparity between an 8x8 and 12x12 state model is negligible, yet the computational effort in the two cases is noticeable. Accordingly an 8x8 model was selected as the baseline for follow up UQ and SA works due to an acceptable balance between computational agreement with experiment and computing resources needed for a converged solution.

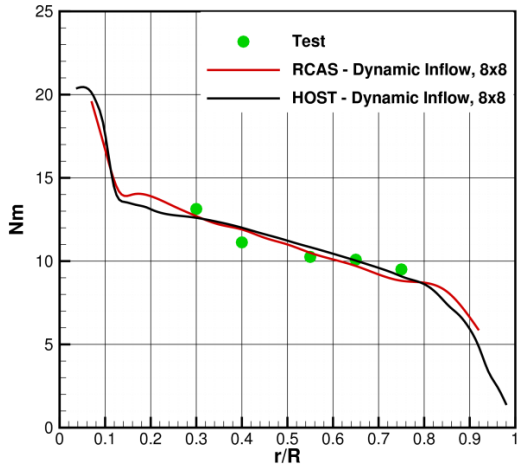

Figure 2: Dynamic inflow model study

5. UNCERTAINTY QUANTIFICATION APPROACH

The forward propagation UQ approach is applied where the probabilistic information on parametric inputs are mapped through the computational model to then assess output statistics. Aleatory uncertainties are considered in this work, hence probability distributions are applied to the input parameters to establish response uncertainties using a probability density function (PDF).

Uncertainty propagation using Monte Carlo simulations is used to define the influence of uncertainties in model inputs on response output. The methodology is used to calculate the uncertainty statistics of the output quantity of interest using a numerical method. In a generalized form, an input parameter, X, is passed through a function evaluator, *f*, which then establishes a measured output, Y, such that:

$$Y = f(X) \quad (1)$$

Where *f* represents the system model; **X** is a vector of uncertain input variables; and **Y** represents a vector of estimated output observations.

The uncertainties in the input variables are represented probabilistically where each component of the input parameter, **X**, is a random variable. Accordingly the system output will also be a random variable, and this randomness is described using PDFs. A MC approach is used to propagate the input uncertainties with a stratified sampling approach that selects data points from the input distributions for analysis by the model. The randomness of the input data points is propagated to the solver using a PDF; then the numerical solver is executed at these points; and the resulting PDF of the outputs subject to the defined input distributions is established.

The merits of the MC approach in obtaining a statistically converged result of the response outputs is limited due to the curse-of-dimensionality of the model inputs. To address this challenge, a response surface model (RSM) is developed and follows two stages. First, an initial sampling of the inputs is formed by the variation of the design space using an optimized Latin Hypercube Sampling (LHS) [7] method. This is then followed by the development of a RSM where the sampled inputs are interpolated using the kriging approach [8]. The advantage of the RSM approach is the computational efficiency since a single evaluation of the model is orders-of-magnitude lower than the CA evaluation time. Accordingly several thousand function evaluations can be efficiently executed to ensure statistical convergence is achieved, and the analysis to follow will demonstrate this process.

Finally, for uncertainty analysis problems with multiple inputs, a global sensitivity analysis (GSA) approach is undertaken using the Sobol indices [9] which are formed using the statistical outputs of the responses due to input variability. To maintain a computationally efficient process, the Sobol indices are computed using the polynomial chaos coefficients which are formed using the RSM approach.

6. WORKFLOW

A generalized form of the computational framework used to support this analysis is presented in Figure 3. At the U.S. Army, one control point is used as a global scaling factor, hence uncertain parameter that acts as a multiplier to the baseline stiffness to uniformly parameterize torsion stiffness from root-to-tip. The analysis is supported with The Design Analysis Kit for Optimization and Terascale Applications (DAKOTA) software [10]. Coupled with DAKOTA are a series of MATLAB functions that support data post-processing that generate output

This work is licensed under the Creative Commons Attribution International License (CC BY). Copyright © 2021 by author(s).

distributions which are then evaluated with performance criteria to determine, for example the likelihood that the system will operate within the specified thresholds. The output statistics including expected value and variance are also established.

Further, the local-UQ framework with HOST at ONERA (right column of Figure 3) uses three control points to generate a non-uniform modification of the torsion stiffness. The control point values induce a modification of the outboard torsion stiffness distribution following an interpolation spline law, as illustrated in Figure 4. In order to ensure that the maximum values are not greater than ±20% of nominal value target, a zero gradient value is imposed at the three control point locations. The choice of considering the outboard section of the blade results from a preliminary study showed that the modification of the inboard section had limited impact on the merit functions of interest. Here, the HOST results are evaluated against available experimental data for the Half Peak-to-Peak (HPP) torsion moment at the experimental measurement location along the blade span. In this setting, the LHS and the kriging are built using an ONERA in-house framework for database and optimization management, and for the sensitivity analysis the OpenTURNS [11] softwar,e co-developed by ONERA, is used. Data post-processing scripts are also formed to establish the statistical metrics and dedicated visualization charts for the uncertainty analysis.

7. NUMERICAL RESULTS

7.1. Parametric study

The primary source of uncertainty that is considered in this analysis is attributed to manufacturing variations which are introduced from sources such as imprecise equipment, varied raw material properties, and heat treatment processes. These variations lead to uncertain performance and may result in compromised parts or decreased service life.

Quantifying the effects of manufacturing variance with metrics such as confidence intervals and error tolerances is an important part of ensuring reliable system performance. In this case, blade deformations due to aerodynamic and structural loads alter the performance characteristics of the rotorcraft. Hence, it is important to investigate the variability in blade stiffness properties and the propagation of the manufacturing variances that ultimately impact flight performance to ensure the aerodynamic and structural loads do not adversely impact flight. To do so, a scaling of bending stiffness between 40% and 200% of the nominal value is modeled for torsional stiffness (GJ). As reference, scaling factor is a uniform multiplier to the nominal baseline stiffness at each node across the span.

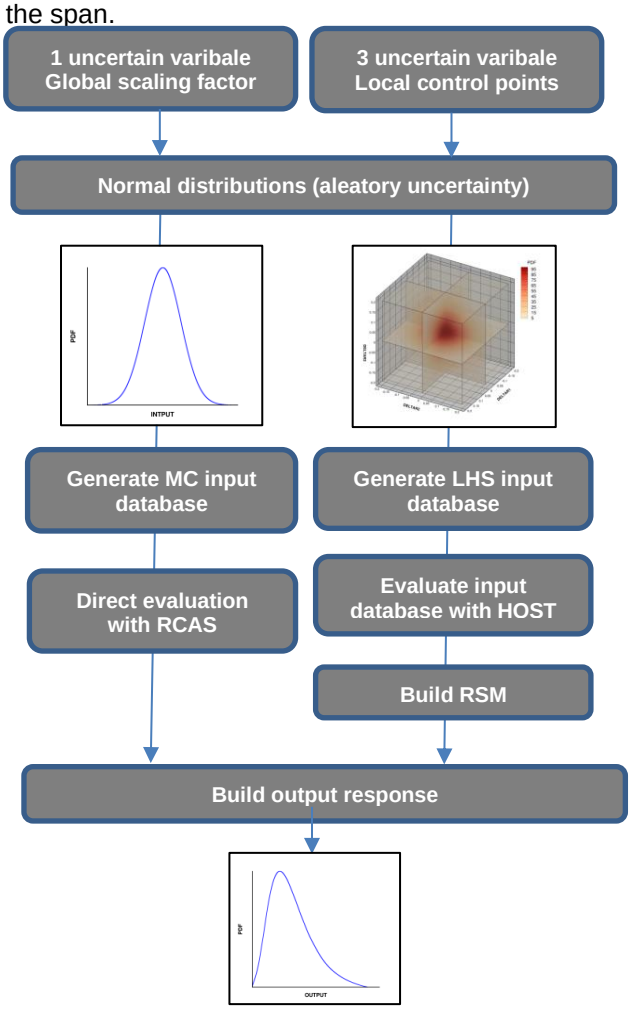

Figure 3: UQ workflow scheme using global (left) and local (right) approaches

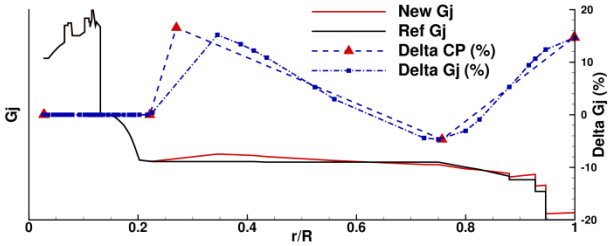

Figure 4: Sample torsion stiffness Gj distribution modification on the outboard by three prescribed control points (CP)

In Figure 5, the analysis shows that there is a significant variation in rotor power with variation of the blade torsional stiffness for the considered scaling values. As the torsional stiffness reduces, there is a higher penalty in rotor performance. The analysis by Jain and Yeo [12] confirmed similar data trends for the UH-60A rotor where it was numerically shown using a coupled CFD/CA analysis that there is a higher drag penalty on the

This work is licensed under the Creative Commons Attribution International License (CC BY). Copyright © 2021 by author(s).

retreating side than on the advancing, and as a result there is an increase in rotor power that is needed to maintain trimmed flight.

As rotor power is sensitive to changes in GJ, its effects with lag and flap stiffness maintained at the nominal baseline values, on maximum torsion moment is modelled in Figure 6. Here, the torsion stiffness is uniformly varied along the span using a SF from 40 to 200% of the baseline values. It can be seen that as the torsional stiffness decreases, there is, in general, a significant increase in the blade structural loads. Similar trends are observed between RCAS and HOST on these outputs.

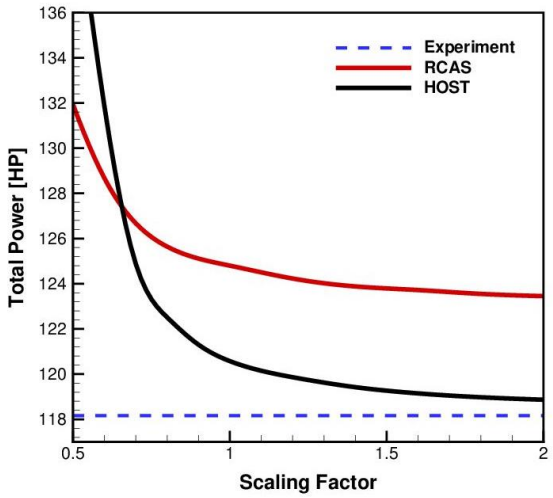

Figure 5: Parametric study as a function of scaling factor on rotor power

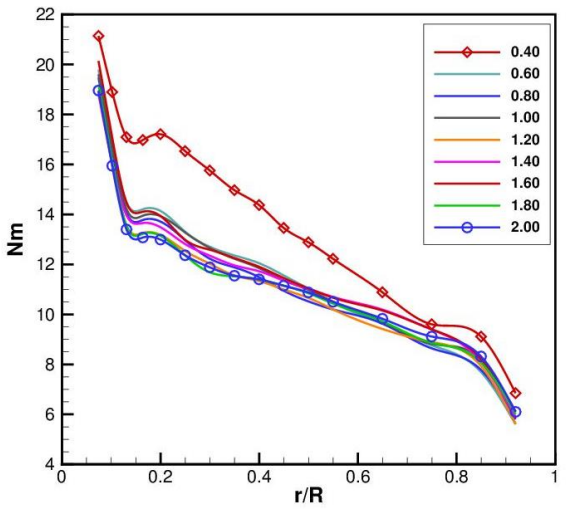

Figure 6: Parametric study as a function of scaling factor on maximum TM using RCAS

As next steps, the uncertainty of GJ on rotor power and peak-to-peak TM amplitude load will form the basis of the UQ and SA analysis.

7.2. Uncertainty Quantification and Propagation analysis

7.2.1. MC based global approach

In this setup, the SF is set as the uncertain parameter and is assumed to be normally distributed. The mean equals one to represent the nominal stiffness setting. To induce variability as part of the uncertainty analysis, the standard deviation is set at 20% about the mean value, hence $\mathcal{N}(1.0,0.20)$. Here, RCAS is executed in the workflow to establish the response outputs of the data points in the sampling population. In the simulations, 1500 RCAS sample points were generated from the input PDF of the SF. Ideally, the simulation sample size must be dynamic to ensure a statistically converged result is established, but to maintain reasonable computing overheads, the maximum number of runs was capped. The sample size utilized in this preliminary analysis will provide an acceptable coverage (although not converged) of the expected data trends which can then be analyzed to assess system uncertainties.

The impact of uncertainty in blade GJ on rotor power and maximum TM is presented in Table 1.

Measure	Baseline	Mean	Std. dev	95% CI
Power [HP]	124.80	125.10	1.40	[124.98,125.22]
Max. TM [Nm]	19.60	19.30	0.38	[19.26,19.33]

Table 1: Representation of normally distributed uniform uncertainty in GJ, $\mathcal{N}(1.0,0.20)$, on rotor power and max. TM using 95% confidence interval – direct Monte Carlo

The impact of GJ on rotor power is outlined in the top row of Table 1. Here it is noted that the converged mean value from the MC simulations is greater than the baseline (baseline represents when stiffness is at the nominal setting or when scaling factor = 1.0). Further, the baseline result is also not within the 95% uncertainty bands. The sensitivity of the variability of GJ on rotor power is expected as per the established patterns in the parametric analysis in Figure 5. The modeled data trend in the tabulated result is attributed to the formation of an asymmetric PDF of rotor power in **Error! Reference source not found.**. For reference, the PDF of the input SF is also presented in Figure 7.

The uncertainty in the material stiffness is induced with a dispersion of SF with a standard deviation of 20% about the baseline stiffness represented by SF_{mean} = 1.0. Figure 7 confirms that from the sampled 1500 data points, the statistical mean for SF matches the input requirement at one (deterministic equals statistical mean). Due to the imposed material stiffness variability, a higher output mean from the MC simulations for power follows at 125.10 HP (statistical mean) relative to baseline (deterministic) at $P_{baseline}$ = 124.80 HP (

This work is licensed under the Creative Commons Attribution International License (CC BY). Copyright © 2021 by author(s).

Figure 8 & Table 1). The PDF for output power is further truncated for Power <≈ 124.00 HP as the modeled cases in the MC simulations were limited to values above this minimum threshold. This further reinforces that statistical convergence has not been achieved, yet the data established will suffice for generalized discussions to be made into the expected uncertainties of the system. Also to be noted is the width of the CI bands which is calculated using the margin-of-error (MoE). At a 95% confidence level, the expected intervals exceed the baseline result. An increase in sample size, n, will reduce the MoE such that the width of the CI bands will converge to the statistical mean, but the mean power will be higher than baseline due to the variability in SF set by a stdev of 20% for GJ. This analysis confirms that with an uncertainty in GJ, the power requirement for trimmed flight will increase, yet the absolute magnitude of the established change is negligible.

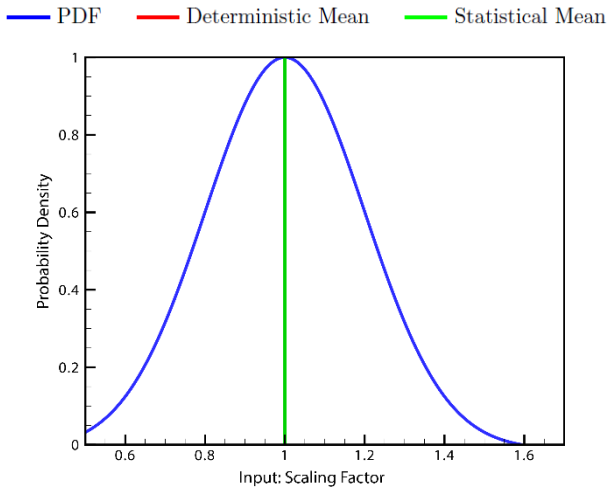

Figure 7: Input PDF, $\mathcal{N}(1.0,0.20)$, for SF

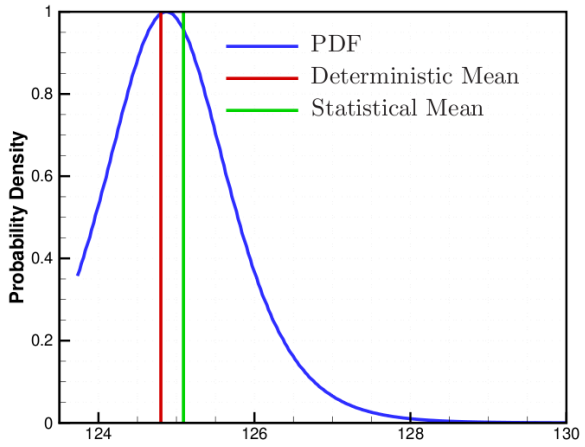

Figure 8 : Output PDF for rotor power [HP]

Further, inferences of extreme deviations in rotor power relative to the median performance due to the stochastic patterns of the sampled GJ data is analyzed. This is processed using a cumulative distribution function (CDF) in Figure 9, where for an assumed critical value of maximum power of 126.00 HP, the probability that rotor power will be less than or equal to this setting due to GJ uncertainty is Pr. (x ≤ 126.00 HP) ≈ 88%.

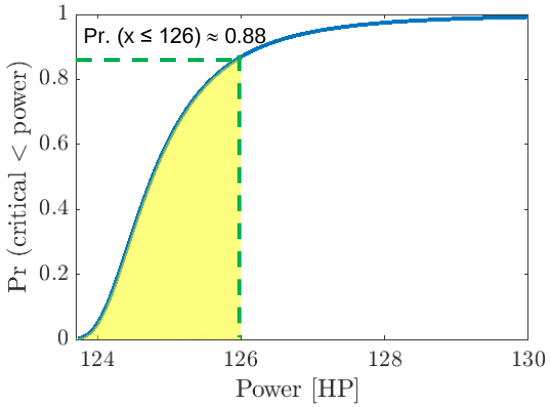

Figure 9: Rotor power CDF due to input GJ uncertainty, $\mathcal{N}(1.0,0.20)$

The information in the CDF provides a probability that a sampled data point lies below a user-defined threshold; the CI in *Table **1*** represents the bands that are likely to contain the true population mean of the system with certain degree-of-confidence. This data can then be used to aid effective decision making for ongoing design refinements if it is determined that system mean performances and/or point estimate probabilities are not within acceptable thresholds and are likely to violate any design requirements. In the case for rotor power, if the probability that the expected power requirement due to GJ uncertainty is likely to exceed the critical setting, then airframe design modifications will be necessary to accommodate a powerplant with higher thrust, hence weight settings. An implementation of a UQ study permits the interpretation of such analysis and facilitates informed decision making.

Further, the analysis of the maximum blade torsion moment due to GJ uncertainty is presented in *Table **1***. The MC mean equals 19.30 Nm which is lower than the baseline value of 19.60 Nm. Further, the nominal result is not in the uncertainty bands using the 95% CI. It is noted that as GJ increases, the torsion frequency also increases, and for the 7A rotor the peak-to-peak TM decreases relative to the baseline setting at SF=1.0. This pattern was further confirmed in the parametric analysis in Figure 6. Accordingly, the uncertainty propagation of GJ confirms that a softer blade relative to baseline will follow at a 95% confidence level leading to the lowering of the peak TM load. Despite these data patterns, the absolute magnitude of the uncertainty relative to the baseline value is negligible as denoted by the narrow 95% CI bands.

This work is licensed under the Creative Commons Attribution International License (CC BY). Copyright © 2021 by author(s).

To further demonstrate the merits of a stochastic-based UQ framework and the information that this approach yields, a CDF is generated in Figure 10. The data is presented by the numerical integration of the PDF to calculate the area under the distribution curve in Figure 9. Here, consider that the maximum $TM_{critical}$ = 19.60 Nm, and the probability that the airframe will experience loads below this threshold such that Pr. ($x \leq 19.60$) due to GJ uncertainty is approximately 80%. Based on this information, critical design decisions can follow if it is determined that the established probability is not within acceptable risk tolerances for the set mission profile.

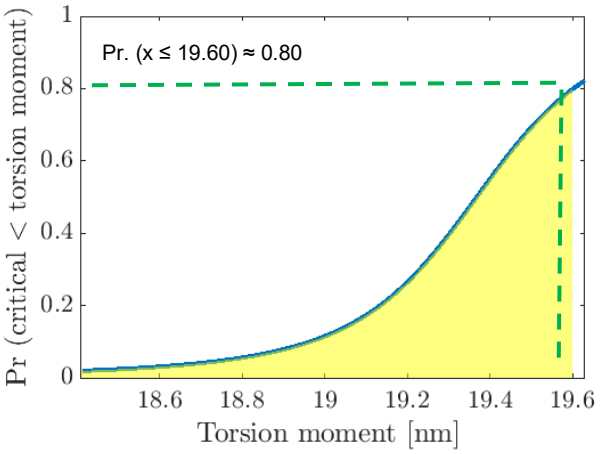

Figure 10: Maximum TM CDF due to input GJ uncertainty, N(1.0,0.20)

7.2.2. RSM based local approach

For the local approach a normal PDF distribution of ±20% variation around the mean value uncertainty distribution is applied to each of the three uncertain input parameters. The resulting distribution is illustrated in Figure 11.

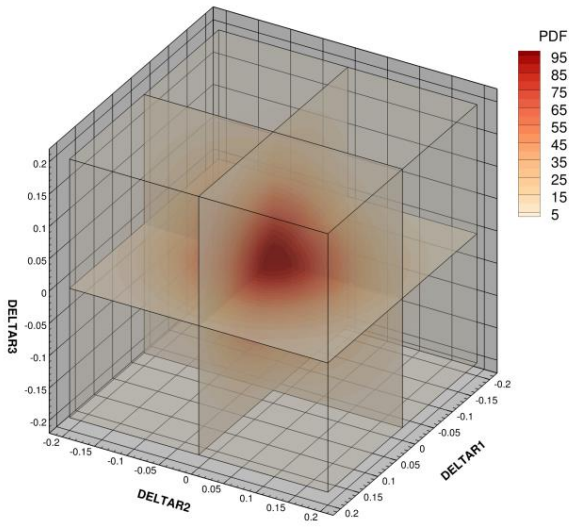

Figure 11: PDF of 3 uncertain inputs following a normal distribution

Here we consider again, as for the global approach, the total power required as well as the torsion moment at the experimental measurement locations. As the observations are evaluated on the response surface model, it was possible to perform a study on the convergence of the input sampling dimension. As shown in Figure 12, a sampling of 10,000 samples is enough to provide converged results from a statistical point of view, which means that the statistical mean variation is negligible as well as the confidence interval value which can be considered small enough. Indeed, the confidence interval is smaller than 0.01% and the statistical mean shows a variation lower than 0.01% too compared with values obtained with 1,000 and 50,000 samples.

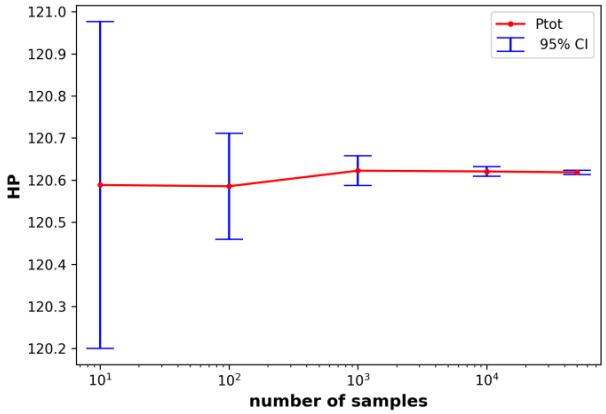

Figure 12: Total power statistical mean and confidence interval convergence history

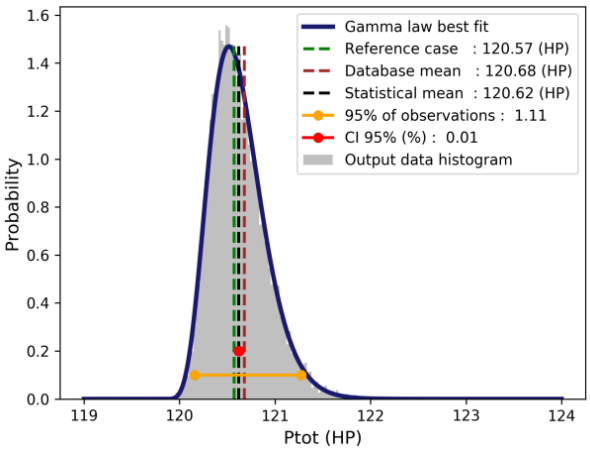

Figure 13: Total power PDF for a 20% variability normally distributed input

Figure 13 provides the total power output PDF with the corresponding statistical data, best fit with a gamma law. This result is very consistent with the PDF obtained with the direct Monte Carlo approach (Figure 8) which indicates that the RCAS and HOST CA tools have very similar behaviour. The statistical mean value is very close to the reference as well as the input database mean values. The uncertainty on

This work is licensed under the Creative Commons Attribution International License (CC BY). Copyright © 2021 by author(s).

the torsion stiffness shows very little impact on the total power variation, as, if we look at the 95% observations range, it remains under 1% of the mean value.

Regarding the CDF (Figure 14), the statistical mean value which is close to the database mean and the reference value are situated at 50% probability. If risk management issues were to be considered, for example the power that is required with a level of confidence of 95%, then the value would be around 121 HP, corresponding to 0.5 HP above the nominal value.

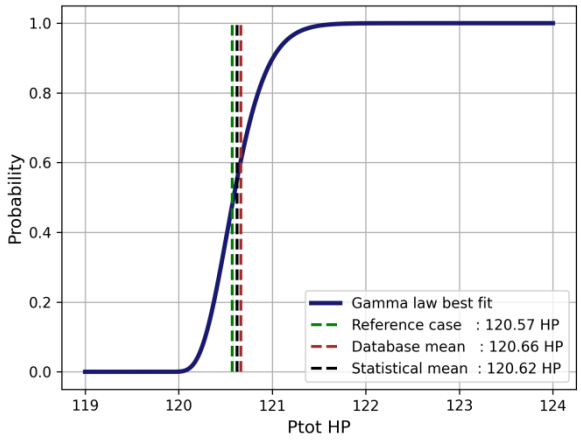

Figure 14: Total power CDF for a 20% variability normally distributed input

A convergence study similar to the one performed for the total power has been performed on the torsion moment values at the experimental data locations. A history chart for the torsion moment half-peak-to-peak statistical data at a sample location is given in Figure 15.

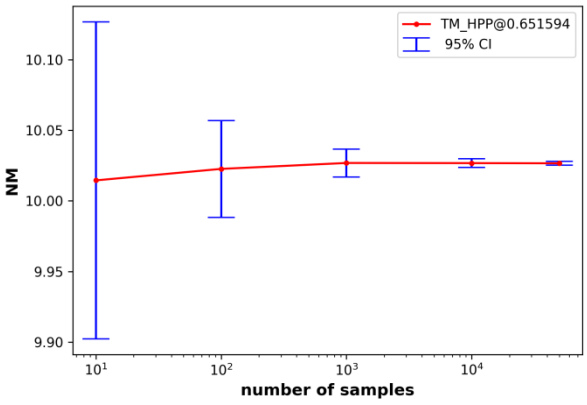

Figure 15: Sample torsion moment HPP at r/R=0,651594 experimental data location statistical mean and confidence interval convergence history

The main results are summarized in Figure 16. The statistical mean value is very close to the reference one. When plotting the 95% range observations, resulting from the output PDF analyses, one can see that for all cases that some observations can reach values closer to the experimental data. If the same statistical metrics were available for the experimental data, which is unfortunately not the case here, we could check if any overlapping occurs.

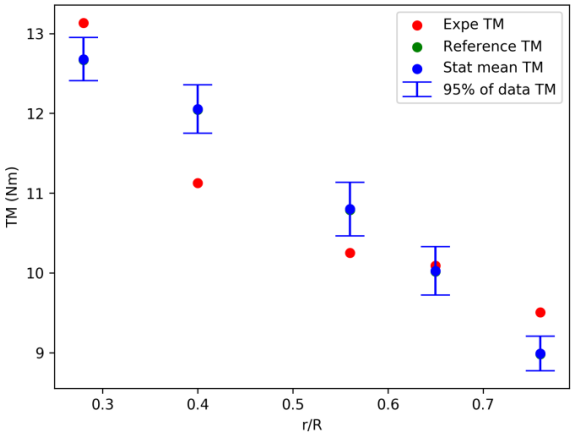

Figure 16: Statistical output for the Torsion Moment at the experimental data measurement location along blade span

The sensitivity analysis using the Sobol indices provides a more quantitative analysis of the relative influence of the three uncertain variables on the total power (Figure 17) and the torsion moments (Figure 18).

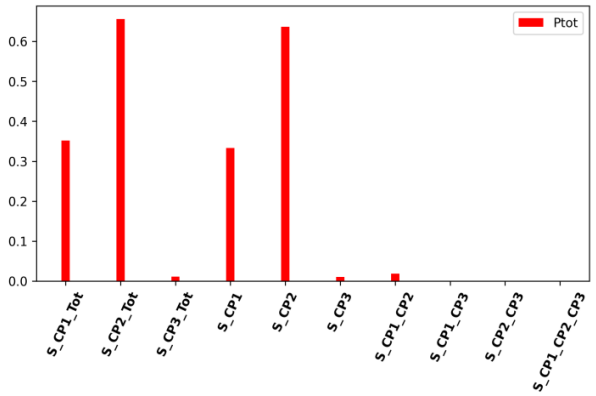

Figure 17 : Sobol indices for total power sensitivity w.r.t. control point uncertain variables

The first, second and third order Sobol indices are provided giving the direct sensitivities as well as the cross sensitivities. It is seen that the second control point is the most influent for all functions of interest. It is followed by the first control point at the inboard station. The only cross sensitivity that plays a non-negligible role is the interaction between the first and second control point for the torsion moment sensitivity.

This work is licensed under the Creative Commons Attribution International License (CC BY). Copyright © 2021 by author(s).

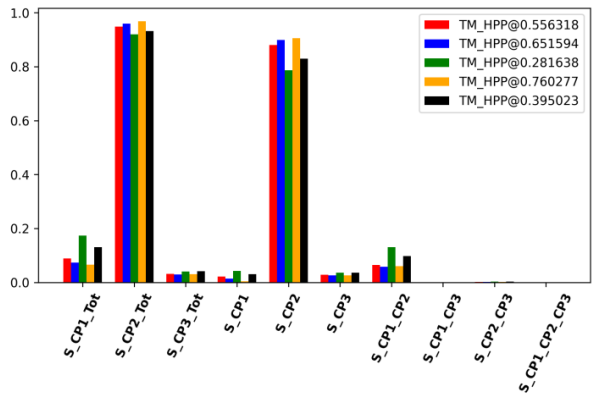

Figure 18 : Sobol indices for torsion moment at experimental data locations w.r.t. control point uncertain variables

8. CONCLUSION

The study focused on the quantification of the uncertainties in rotor power and torsion moment in its maximum and local half-peak-to-peak values due to input variability in blade torsion stiffness. A global and local-based uncertainty approach was applied using automated workflows and processes coupled with validated comprehensive analysis tools. The global approach utilized the MC framework and the local method integrated a RSM to enhance the computational efficiency. The outputs to a stochastic-based approach were analyzed using a statistical framework. The MC analysis confirmed that uncertainty propagation of torsion stiffness has negligible impact on rotor power and maximum torsion moment along the blade span. Even if the RSM approach confirmed the robustness of the power performance with respect to the torsion stiffness variability, it further showed that the uncertainty in torsion stiffness could explain partly the difference between the numerical and the experimental values. It also helped, through the sensitivity analysis, identifying the most influent uncertain parameters as well as the cross sensitivities.

The computational methods proposed in this works demonstrated the role of UQ and SA tools for rotorcraft applications. The complexity of the problem proposed in this works will be extended further to further enhance and demonstrate the concepts and merits of this work respectively in addressing multi-dimensional real life problems that are relevant to rotorcraft aeromechanics. This will involve incorporating additional uncertain input parameters including flap and lag stiffness and their combined effects on rotor aeroelastic behaviour including maximum torsion, flap and chord bending moments, including total rotor power. The uncertainties in the spanwise bending moment loads also need to be quantified. Furthermore, from a UQ perspective, model form uncertainties with epistemic variables in the CA toolset (RCAS and HOST) need to be identified and integrated into the analysis so that the combined effects with the identified aleatory parameters can be established on the response outputs. Through this effort, sensitivity analysis will provide critical information on the input parameters that yield high output uncertainties, hence informed design decisions can follow to mitigate the effects of these parameters on output variability.

9. BIBLIOGRAPHY

[1] B. Benoit, A. Dequin, K. Kampa, W. Grunhagen, P. Basset and B. Gimonet, "HOST, a General Helicopter Simulation Tool for Germany and France," in *56th Annual Forum of the American Helicopter Society*, Virginia Beach, VA, May 2-4, 2000.

[2] H. Saberi, M. Hasbun, J. Y. Hong, H. Yeo and R. A. Ormiston, "Overview of RCAS Capabilities Validations, and Rotorcraft Applications," in *American Helicopter Society 71st Annual Forum*, Virginia Beach, VA, May 5-7, 2015.

[3] B. Ortun, M. Potsdam, H. Yeo and K. Truong, "Rotor Loads Prediction on the ONERA 7A Rotor using Loose Fluid/Structure Coupling," *Journal of the American Helicopter Society,* vol. 62, no. 3, July, 2017.

[4] P. Beaumier, M. Costes, B. Rodriguez, M. Poinot and B. Cantaloube, "Weak and Strong Coupling between the elsA CFD solver and the HOST Helicopter Comprehensive analysis," in *31st European Rotorcraft Forum*, Florence, Italy, September 13-15, 2005.

[5] H. Yeo, M. Potsdam, B. Ortun and K. Truong, "High-Fidelity Structural Loads Analysis of the ONERA 7A Rotor," *Journal of Aircraft,* vol. 54, no. 5, September-October 2017.

[6] K. Pahlke and B. G. van der Wall, "Chimera Simulations of Multibladed Rotors in High-Speed Forward Flight with Weak Fluid-Structure Coupling," *Aerospace Science and Technology,* vol. 9, no. 5, July, 2005.

[7] R. J. B. a. W. J. C. M. D. McKay, "Comparison of three methods for selecting values ofinput variables in the analysis of output from a computer code," *Technometrics,* vol. 21, no. 2, p. 239–245, 1979.

[8] D. G. Krige, ".A Statistical Approach to Some Mine Valuation and Allied Problems on the

This work is licensed under the Creative Commons Attribution International License (CC BY). Copyright © 2021 by author(s).

Witwatersrand.," *Master's thesis, University of Witwatersrand,* 1951.

[9] I. Sobol, "Global sensitivity indices for nonlinear mathematical models and their monte carlo estimates.Mathematics and Computers in Simulation," *The Second IMACS Seminar on MonteCarlo Methods,* vol. 55, no. 1, p. 271–280, 2001.

[10] B. e. a. Adams, "Dakota, A Multilevel Parallel Object-Oriented Framework for Design Optimization, Parameter Estimation, Uncertainty Quantification, and Sensitivity Analysis: Version 6.12 User's Manual," *Sandia Technical Report SAND2020-12495,* 2020.

[11] D. A. a. P. A.-L. Iooss B. Baudin M., "Open turns: An industrial software for uncertaintyquantification in simulation," *Handbook of Uncertainty Quantification,* 2015.

[12] R. Jain and H. Yeo, "Effects of torsion frequencies on rotor performance and structural loads with trailing edge flap," *Smart Material Structures,* vol. 21, no. 8, August 2012.

This work is licensed under the Creative Commons Attribution International License (CC BY). Copyright © 2021 by author(s).